

# Physicochemical Investigation of 2,4,5-Trimethoxybenzylidene Propanedinitrile (TMPN) Dye as Fluorescence off-on Probe for Critical Micelle Concentration (CMC) of SDS and CTAB

Salman A. Khan<sup>1</sup> · Abdullah M. Asiri<sup>1,2</sup>

Received: 1 June 2015 / Accepted: 14 September 2015  
© Springer Science+Business Media New York 2015

**Abstract** 2,4,5-trimethoxybenzylidene propanedinitrile (TMPN) was synthesized by Knoevenagel condensation. Structure of the TMPN was confirmed by the elemental analysis and EI-MS, FT-IR, <sup>1</sup>H-NMR, <sup>13</sup>C-NMR spectroscopy. Absorbance and emission spectrum of the TMPN was studied in different solvent provide that TMPN is good absorbent and emission red shift in absorbance and emission spectra as polarity of the solvents increase. Photophysical properties including, oscillator strength, extinction coefficient, transition dipole moment, stokes shift and fluorescence quantum yield were investigated in order to investigate the physicochemical behaviors of TMPN. Dye undergoes solubilization in different micelles and may be used as a probe to determine the critical micelle concentration (CMC) of SDS and CTAB.

**Keywords** TMPN · Dipole moment · Fluorescence quantum yield · CMC · SDS · CTAB

## Introduction

Long chain pi bond conjugated system is known as chromophore. Organic compound containing with chromophores are

responsible for the color because molecules absorbs the visible light at certain wavelength [1]. Various food colorings dyes, pigments, cotton fabric dyes, pH-indicators, lycopene, stains and  $\beta$ -carotene all contain chromophores [2, 3]. Donor and acceptor group such as N-(CH<sub>3</sub>)<sub>2</sub>, OCH<sub>3</sub>, OH and CN, NO<sub>2</sub> can easily give the lone pair of electron to the acceptor [4]. Intramolecular charge-transfer (ICT) of molecules are formed between a donor (D) group and an acceptor (A) group in the ground states or excited states [5]. ICT molecules have unique absorption bands in the region of ultraviolet–visible spectra [6]. Due to this behavior donor–acceptor containing chromophores have attracted current interests in terms of materials science such as near-infrared dyes, nonlinear optics, photonic imaging, electrochemical sensing, langmuir films, photoinitiated polymerization, dye synthesis solar cell [7–9]. Photophysical and Physicochemical studies such as, oscillator, fluorescent quantum yield strength, solvatochromic, piezochromic, and photostability are one of most important studies to determine the physicochemical behavior of the molecules [10]. Numerous reactions were reported for the synthesis of donor–acceptor chromophores [11, 12]. However, Knoevenagel condensation is one of the most imperative reactions for the development of donor acceptor chromophores by the reaction of carbonyl compounds with active methylene carbon in the presence of some Lewis acids or Lewis base followed by a nucleophilic addition and dehydration reaction [13]. Different synthetic methods were reported for Knoevenagel reaction, such as normal/refluxing in the solvent [14], ultrasonication, microwave radiation [15], solid-phase reaction [16] and photosensitization [17]. Due to numerous application of donor acceptor chromophores and continues work on the photophysical studies in this paper we are reporting the synthesis of donor acceptor chromophore 2,4,5-trimethoxybenzylidene propanedinitrile (TMPN) and its photophysical investigation.

✉ Salman A. Khan  
sahmad\_phd@yahoo.co.in

<sup>1</sup> Chemistry Department, Faculty of Science, King Abdulaziz University, P.O. Box 80203, Jeddah 21589, Saudi Arabia

<sup>2</sup> Center of Excellence for Advanced Materials Research, King Abdulaziz University, P.O. Box 80203, Jeddah 21589, Saudi Arabia

## Experimental

### Chemicals and Reagents

The 2,4,5-trimethoxybenzylidene and malononitrile were acquired from Acros Organic. All solvents and reagents (A.R.) were acquired commercially and utilized with no additional purification, excluding dimethylformamide (DMF), ethanol and methanol.

### Apparatus

Thomas Hoover capillary melting apparatus was used to record the melting points of the synthesized compounds without any correction. Nicolet Magna 520 FT-IR spectrometer was utilized to record the FT-IR spectra. Bruker DPX 600 MHz spectrometer with tetramethyl silane as internal standard at room temperature was used to perform the  $^1\text{H}$ -NMR and  $^{13}\text{C}$ -NMR experiments in  $\text{CDCl}_3$ . Shimadzu UV-160A spectrophotometer was utilized to gain the UV-Vis electronic absorption data and by using a 10 mm quartz cell absorption spectra were collected. By using Shimadzu RF 5300 spectrofluorophotometer having a quartz cell of rectangular shape with dimensions  $0.2\text{ cm} \times 1\text{ cm}$  for minimizing the reabsorption. Emission spectra were observed at right angle. Before proceeding data analyses, all fluorescence spectra were blank subtracted.

### Synthesis of 2,4,5-Trimethoxybenzylidene Propanedinitrile (TMPN)

A mixture of the 2,4,5-trimethoxybenzylidene (0.025 mol, 0.5 g) and malononitrile (0.025 mol) in absolute ethanol (25 mL) of few drop of pyridine was refluxed at  $80^\circ\text{C}$  for 3 h with continuous stirring. The reactions were monitored through TLC using solvent system ethyl acetate: benzene (2:8), when the reaction was found to be complete, then reaction mixture was cooled in an ice bath and the product thus formed was filtered washed with water and recrystallized by distilled ethanol and chloroform. Mp.  $166^\circ\text{C}$ ; Yield: 75 %; IR (KBr)  $\nu_{\text{max}}\text{ cm}^{-1}$ : 3030 (C-H), 2930 (C-H), 2220 (C-CN), 1570 (C=C);  $^1\text{H}$ -NMR ( $\text{CDCl}_3$ )  $\delta$ : 8.14 (s, CH), 7.78 (s, 1H, CHAromatic), 7.19 (s, 1H, CHAromatic), 3.93 (s, 3H,  $\text{OCH}_3$ ), 3.85 (s, 3H,  $\text{OCH}_3$ ), 3.02 (s, 3H,  $\text{OCH}_3$ );  $^{13}\text{C}$ -NMR ( $\text{CDCl}_3$ )  $\delta$ : 156.85, 156.52, 152.53, 143.57, 115.36, 114.49, 112.23 C-Aromatic, 95.44, 77.04, 76.83, 75.66, 56.49 ( $\text{OCH}_3$ ), 56.37 ( $\text{OCH}_3$ ), 56.39 ( $\text{OCH}_3$ ); EI-MS  $m/z$  (rel. int.%): 246 (76)  $[\text{M}+1]^+$ ; Anal. calc. for  $\text{C}_{13}\text{H}_{12}\text{N}_2\text{O}_3$ : C, 63.93, H, 4.95, N, 11.47, Found: C, 63.90, H, 4.92, N, 11.43.

The fluorescence quantum yield ( $\phi_f$ ) was measured using the optically diluted solution to avoid reabsorption effect (absorbance at excitation wavelength  $\leq 0.1$ ), relative method with solution of quinine sulfate in  $0.5\text{ mol dm}^{-3}\text{ H}_2\text{SO}_4$  ( $\phi = 0.55$ ),

using the same excitation wavelength, the unknown quantum yield is calculated using the following Eq. (1).

$$\Phi_f = \Phi_r \frac{I_s \times A_r \times n_s^2}{I_r \times A_s \times n_r^2} \quad (1)$$

where  $\phi$  is the quantum yield,  $I$  is the integrated emission intensity,  $A$  is the absorbance at excitation wavelength, and  $n$  is the refractive index of the solvent. The subscript  $r$  refers to the reference fluorophore of known quantum yield [18]. The photochemical quantum yield ( $\phi_c$ ) was calculated using the method that was described in details previously [19].

## Result and Discussion

### Chemistry

The synthesis of 2,4,5-trimethoxybenzylidene propanedinitrile (TMPN) is straight forward and the TMPN was isolated in good yield. [18] The acquired TMPN is stable in both solid as well as in the solution form. The structure of synthesized compound shown in experimental section was recognized by comparing spectral data  $^1\text{R}$ ,  $^1\text{H}$ -NMR &  $^{13}\text{C}$ -NMR. It is clear from the IR band positions that the formation of the TMPN takes place. TMPN demonstrated intense bands at  $1570\text{ cm}^{-1}$  due to  $\nu(\text{C}=\text{C})$  stretch, which proves the formation of TMPN by konovelgal; condensation. Additional confirmation for the formation of TMPN was acquired from the  $^1\text{H}$ -NMR spectra, which offer diagnostic tools for the positional illumination of the protons. Assignments of the signals are based on the chemical shifts and intensity patterns. The aromatic protons of TMPN is shown as two singlet ( $s$ ) at 7.78 and 7.19 ppm. A Singlet due to  $=\text{C}-\text{H}$  proton in the TMPN at 8.14 ppm was observed at respectively.

$^{13}\text{C}$  NMR ( $\text{CDCl}_3$ ) spectra of TMPN was recorded in  $\text{CDCl}_3$  and spectral signals are in good agreement with the probable structures details of  $^{13}\text{C}$ -NMR spectra of TMPN and data are given in the experimental section. Finally characteristic peaks were observed in the mass spectra of TMPN by the molecular ion peak. The mass spectrum of TMPN shows a molecular ion peak ( $\text{M}^+$ )  $m/z$  246.

### Spectral behavior of 2,4,5-Trimethoxybenzylidene Propanedinitrile (TMPN)

UV-vis electronic spectra of TMPN in ten organic solvent with different polarities were studied. UV-vis absorption spectra of the studied TMPN was measured in various non-polar, polar aprotic and polar protic solvents such as ethanol, methanol, dimethylsulfoxide, dimethylformamide, chloroform, dichloromethane, carbon tetrachloride, acetonitrile, dioxan, tetrahydrofuran. Fig. 1 shows absorption spectra of  $1 \times 10^{-5}\text{ mol dm}^{-3}$

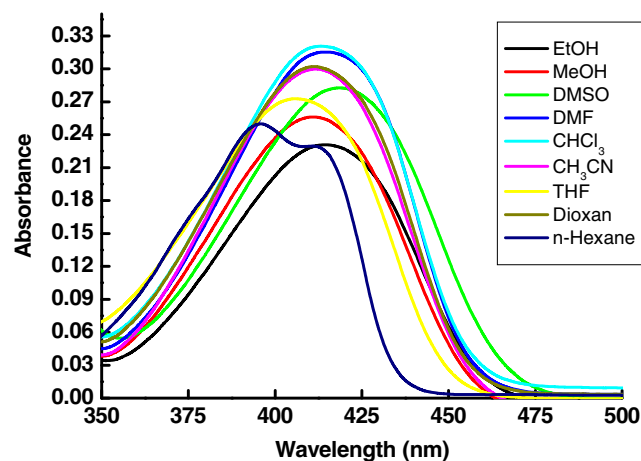


**Fig. 1** Electronic absorption spectra of  $1 \times 10^{-5}$  mol  $\text{dm}^{-3}$  of TMPN in different solvents

solution of TMPN in these solvents as a sample. As it can be seen from Fig. 1, in the all solvent tested the main band of TMPN, located in the spectral range 395–421 nm. Shorter wavelength band in UV region observed for studies TMPN in different solvent system is assigned to  $\pi$  to  $\pi^*$  transition of the benzenoid system toward the  $\text{OCH}_3$  which is characterized by high electron donation and nitrile electron group is accepting character present in its structure. The emission spectra, however, are broad and red shifted (Fig. 2) as the solvent polarity increases. The red-shift from 446–503 nm in n-Hexane to in DMSO indicates that photoinduced intramolecular charge transfer (ICT) occurs in the singlet excited state [19] and therefore the polarity of TMPN increases on excitation. The red shift of the fluorescence peak in alcoholic solvents are assigned to solute – solvent hydrogen bonding interaction in the singlet excited state which causes an extra red shift in the observed spectra [20] (Table 1).

A simplified description of hydrogen bonding of TMPN is shown in Scheme 1 Type (a) hydrogen bonding is strengthened in the excited state, since the charge density at the nitrile

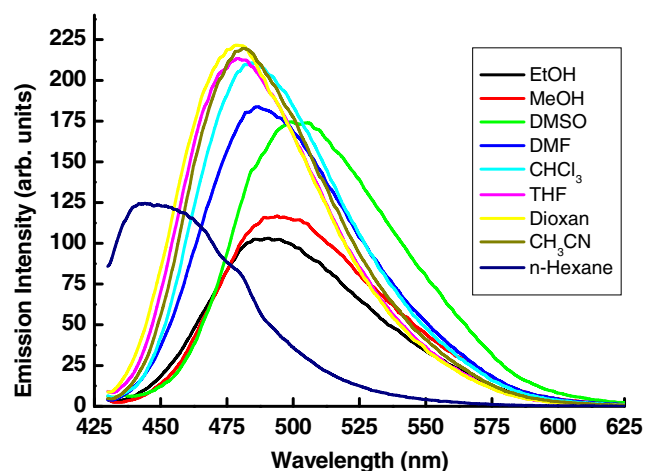


**Fig. 2** Emission spectra of  $1 \times 10^{-5}$  mol  $\text{dm}^{-3}$  of TMPN in different solvents

nitrogen is enhanced in the ICT excited state. On the other hand, type (b) hydrogen bonding is weakened on photoexcitation, because the charge densities at the  $\text{OCH}_3$  decrease in the excited state.

The energy of absorption ( $E_a$ ) and emission ( $E_f$ ) spectra of the TMPN in different solvents correlated with the empirical Dimroth polarity parameter  $E_T(30)$  [21] of the solvent (Fig. 3). A linear correlation between the energy of absorption and emission versus polarity of solvents was obtained (Eqs. 1 and 2), implying potential application of these parameters to probe the microenvironment of TMPN.

$$E_a = 75.17 - 0.1032 \times E_T(30) \quad (2)$$

$$E_f = 68.28 - 0.257 \times E_T(30) \quad (3)$$

### Determination of Oscillator Strength and Transition Dipole Moment

The solvatochromic performance of TMPN allows to establish the difference in the dipole moment between the excited singlet and the ground state ( $\Delta\mu = \mu_e - \mu_g$ ). This variation can be obtained using the simplified Lippert–Mataga equation as follows [21, 22]:

$$\Delta\bar{\nu}_{st} = \frac{2(\mu_e - \mu_g)^2}{hca^3} \Delta f + \text{Const.} \quad (4)$$

$$\Delta f = \frac{D-1}{2D+1} - \frac{n^2-1}{2n^2+1} \quad (5)$$

where  $\Delta\bar{\nu}_{st}$  is known as Stokes-shift which decreasing with decreasing the solvent polarity indicating to weak stabilization of the excited state in non polar solvents [21].  $\Delta f$  is the orientation polarizability of the solvent,  $\mu_e$  and  $\mu_g$  are the dipole moments in the excited and ground state, respectively which measures both electron mobility and dipole moment of the solvent molecule.  $c$  is the speed of light in vacuum,  $a$  is the Onsager cavity radius and  $h$  is Planck's constant,  $n$  and  $\epsilon$  are the refractive index and dielectric constant of the solvent for Eq. 4 respectively. The Onsager cavity radius was chosen to be 4.2 Å because this value is comparable to the radius of a typical aromatic fluorophore [23].

$\Delta\bar{\nu}_{ss}$  is the Stokes shifts of the TMPN in different solvents were deliberate, as shown in Table 1, using the following the equation [24]:

$$\Delta\bar{\nu}_{ss} = \bar{\nu}_{ab} - \bar{\nu}_{em} \quad (6)$$

where  $\Delta\bar{\nu}_{ss}$  is the difference between  $\lambda_{\text{max}}$  of the  $\bar{\nu}_{ab}$  and  $\bar{\nu}_{em}$  indicate the wavenumbers of absorption and emission maxima ( $\text{cm}^{-1}$ ) respectively.

**Table 1** Spectral data of TMPN in different solvents

Solvent	$\Delta f$	$E_T^N$	$E_T$ (dye)	$\lambda_{ab}(nm)$	$\lambda_{em}(nm)$	$\epsilon$ $M^{-1}cm^{-1}$	$f$	$\mu_{12}$ Debye	$\Delta\nu$ ( $cm^{-1}$ )	$\Phi_f$
EtOH	0.305	0.94	68.72	416	494	23000	0.33	5.39	3672	0.32
MeOH	0.308	1.19	69.39	412	490	25600	0.39	5.83	3863	0.34
DMSO	0.266	1.14	67.91	421	503	28060	0.43	6.19	3872	0.47
DMF	0.263	1.16	68.56	417	486	31300	0.42	6.09	3404	0.43
$CHCl_3$	0.217	1.18	69.22	413	484	32100	0.45	6.27	3552	0.49
Acetonitrile	0.274	1.19	69.39	412	482	29800	0.42	6.05	3525	0.57
Dioxan	0.148	1.20	69.73	410	479	30400	0.42	6.04	3514	0.56
THF	0.263	1.22	70.24	407	476	27000	0.42	6.01	3562	0.56
n-Hexane	0.0014	1.28	72.38	395	446	24700	0.42	4.84	2895	0.36

The change in dipole moments ( $\Delta\mu$ ) between the excited singlet and ground state were calculated from the slope of plot of Stokes shifts ( $\Delta\nu_{ss}$ ) and orientation polarizability of the solvent ( $\Delta f$ ) as 5.58 debye for TMPN respectively, positive value indicating that the excited state is more polar than the ground state.

The change in transition dipole moments ( $\Delta\mu_{12}$ ) between the excited singlet and ground state of TMPN in various solvents were calculated as in Table 1, using the Eq. 7 [25].

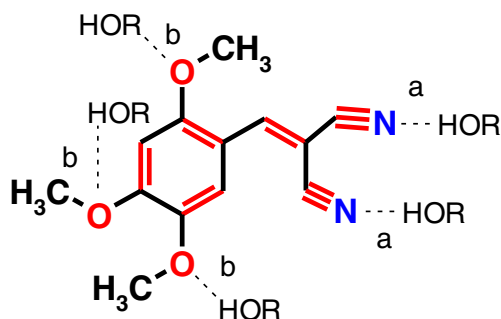
$$\mu_{12}^2 = \frac{f}{4.72 \times 10^{-7} \times E_{max}} \quad (7)$$

where  $E_{max}$  is the maximum energy of absorption in  $cm^{-1}$  and  $f$  is the oscillator strength.

The oscillator strength ( $f$ ), can be calculated using the following equation:

$$f = 4.32 \times 10^{-9} \int \epsilon(\bar{\nu}) d\bar{\nu} \quad (8)$$

where  $\bar{\nu}$  represents the numerical value of wavenumber ( $cm^{-1}$ ) and  $\epsilon$  is the extinction coefficient ( $Lmol^{-1}cm^{-1}$ ).

**Scheme 1** (TMPN)

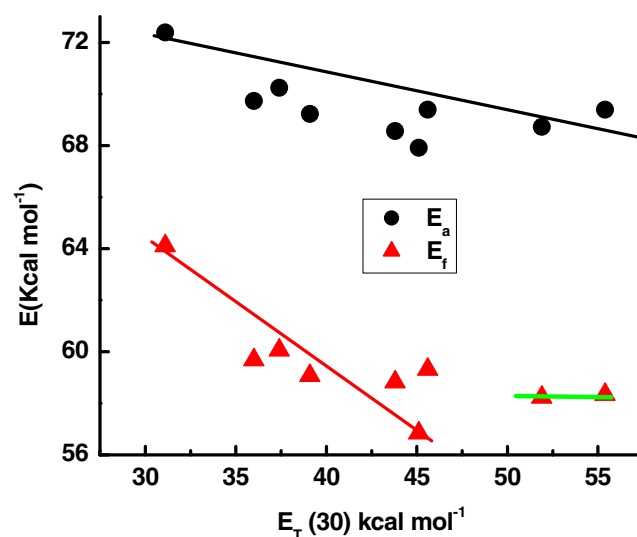
Oscillator strength values of TMPN in various solvents were calculated from the Eq. 8 and reported in Table 1, [26].

$E_T(30)$  and  $E_T^N$  is the empirical Dimroth polarity parameter of TMPN was also premeditated according to the following equation [27].

$$E_T^N = \frac{E_T(\text{solvent}) - 30.7}{32.4} \quad (9)$$

$$E_T(\text{solvent}) = \frac{28591}{\lambda_{max}} \quad (10)$$

where  $\lambda_{max}$  corresponds to the peak wavelength (nm) in the red region of the intramolecular charge transfer absorption of the bitain dye. TMPN has bathochromic when solvent polarity increase from n-hexane to DMSO indicates that the polarity of TMPN and photo-induced intramolecular charge transfer (ICT) occurs in

**Fig. 3** Plot of energy of absorption ( $E_a$ ) and emission ( $E_f$ ) versus  $E_T(30)$  of different solvents

the singlet excited state, therefore increasing the excitation(Fig. 4).

### Fluorescence Quantum Yield

The fluorescence quantum yield ( $\phi_f$ ) of TMPN depends strongly on the solvent properties (Table 1). The fluorescence quantum yield can be correlated with  $E_T(30)$  of the solvent, where  $E_T(30)$  is the solvent polarity parameter introduced by Reichardt [28] Fig. 5. The fluorescence quantum yield of TMPN increases with increasing solvent polarity from 0.36 in a non-polar solvent n-Hexane to 0.57 in a moderately polar solvent acetonitrile; with a further increase in solvent polarity the fluorescence quantum yield seems to decrease, i.e., 0.32 in a strongly polar solvent,  $C_2H_5OH$ . The fluorescence quantum yield of TMPN varied between 0.36 in n-Hexane, 0.57 in acetonitrile and 0.32 in  $C_2H_5OH$  solvent. This indicates the occurrence of negative solvatokinetic effect and positive solvatokinetic effect [29] during the course of increasing solvent polarity. One main reason for the negative solvatokinetic effect (increase  $\phi_f$  with a suitable enhancement of ICT) could be due to the biradicaloid charge transfer involving the unbridged double bonds and the other cause could be related to the proximity effect for compounds with  $n-\pi^*$  and  $\pi-\pi^*$  electron configuration. In other words, in non-polar solvents, these effects will result in effective nonradiative decay of the excited states. In strong polar solvents, the fluorescence quantum yield decreases, due to large degree of intramolecular charge transfer, which causes an increase in the rate of radiationless relaxation of an excited state, giving rise to positive solvatokinetic effect (reduction in  $\phi_f$  by strong ICT). Moreover, the much lower fluorescence quantum yields in proton solvents can be attributed to the hydrogen bond interaction between the molecule and surrounding solvent, which

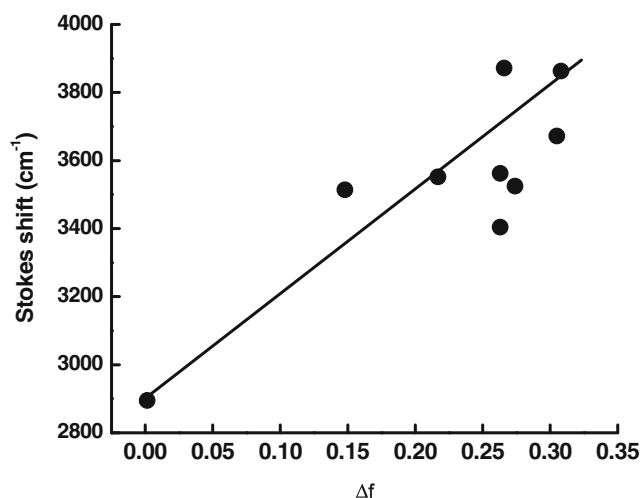


Fig. 4 Plot of  $\Delta F$  versus Stokes shift ( $\Delta\nu$ )

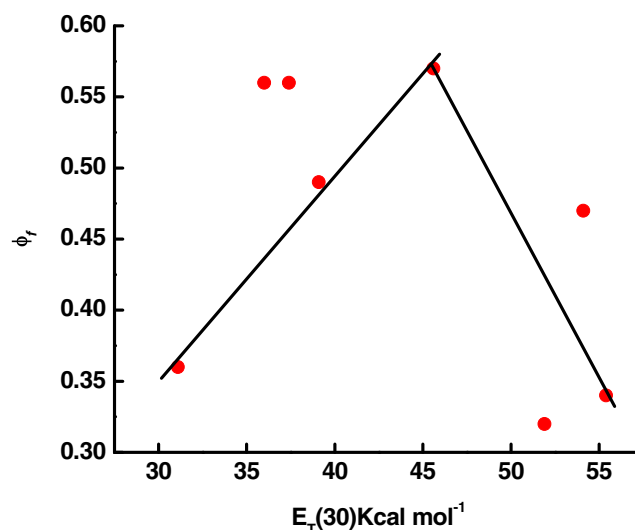


Fig. 5 Plot of  $\phi_f$  versus  $E_T(30)$  of different solvents

results in an additional nonradiative decay as observed in other dipolar molecules.

### Effect of Surfactant on Emission Spectrum of TMPN

A positively charged and cetyltrimethyl ammonium bromide (CTAB) and negatively charged sodium dodecyl sulphate (SDS) surfactants were selected for evaluating the emission behavior of the TMPN dye. The two specified surfactants were chosen because ionic charges possessed by TMPN dye can be influenced by the positively charged CTAB and negatively charged SDS. Thus, the charge attraction accounts for the TMPN emission behavior. Fluorescence emission spectra of TMPN in the absence and presence of CTAB and SDS were measured. Fluorescence intensities of TMPN increase when increasing the concentration of CTAB from  $2 \times 10^{-4}$  up to  $1.6 \times 10^{-3}$  M as shown Fig. 6. Such enhancement in the fluorescence intensity of  $1 \times 10^{-5}$  M TMPN at fixed concentrations with an increase in the CTAB concentration may likely be ascribed to the association mechanism of TMPN with CTAB. The fluorescence intensity of TMPN is quenched with an increase of the SDS concentration ( $2 \times 10^{-3}$  up to  $1.6 \times 10^{-2}$  M). Moreover, more significant reductions were noticed in fluorescence intensities of TMPN with SDS. The quenching of TMPN upon increasing SDS concentration can likely be ascribed to the association of TMPN with SDS. Fig. 7 represents the influence of SDS on the relative emission intensity of  $1 \times 10^{-5}$  M TMPN. It can be observed that there was a subsequent decrease in the relative emission intensity of TMPN with an increase in the SDS concentration, strongly providing that there was an interaction between TMPN and SDS. It seems that the dye molecules located in the hydrocarbon core of CTAB aggregates, while in SDS, the dye located at micelle – water interface, with quenching role of water. As shown in Figs. 6 and 7, the emission intensity of TMPN



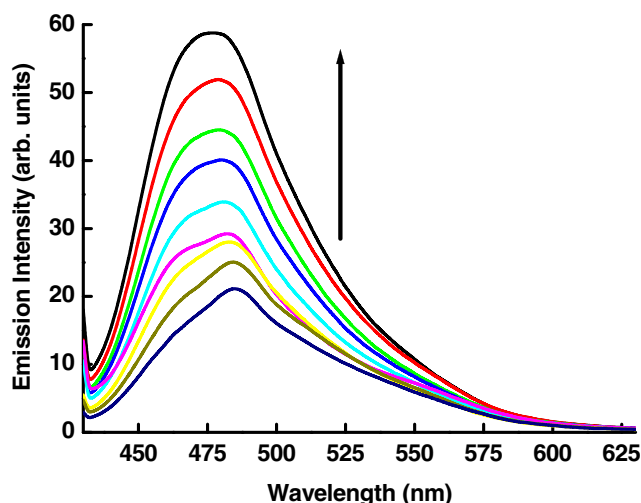


**Fig. 6** Emission spectrum of  $1 \times 10^{-5}$  mol  $\text{dm}^{-3}$  of TMPN at different concentrations of CTAB, the concentrations of CTAB at increasing emission intensity are  $0.0$ ,  $2 \times 10^{-4}$ ,  $4 \times 10^{-4}$ ,  $6 \times 10^{-4}$ ,  $8 \times 10^{-4}$ ,  $10 \times 10^{-4}$ ,  $12 \times 10^{-4}$ ,  $16 \times 10^{-4}$  and  $18 \times 10^{-4}$  mol  $\text{dm}^{-3}$

increases with increasing the concentration of surfactant CTAB, and emission intensity of TMPN decreases with increasing the concentration of surfactant SDS an abrupt change in fluorescence intensity is observed at surfactant concentration of  $8.21 \times 10^{-4}$  and  $6.10 \times 10^{-3}$  mol  $\text{dm}^{-3}$  which are very close to the critical micelle concentration of CTAB and SDS [30], thus TMPN can be employed as a probe to determine the CMC of a surfactants Figs. 8 and 9. It was well known that aromatic molecules were generally solubilized in the palisade layer of micelle [31, 32]. Thus the enhancement of emission intensity is attributed to the passage of dye molecule from the

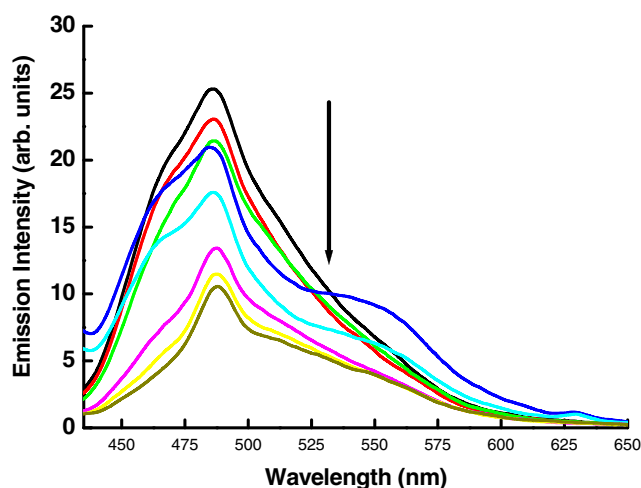


**Fig. 7** Emission spectrum of  $1 \times 10^{-5}$  mol  $\text{dm}^{-3}$  of TMPN at different concentrations of SDS, the concentrations of SDS at decreasing emission intensity are  $0.0$ ,  $2 \times 10^{-3}$ ,  $4 \times 10^{-3}$ ,  $6 \times 10^{-3}$ ,  $8 \times 10^{-3}$ ,  $10 \times 10^{-3}$ ,  $12 \times 10^{-3}$  and  $16 \times 10^{-3}$  mol  $\text{dm}^{-3}$

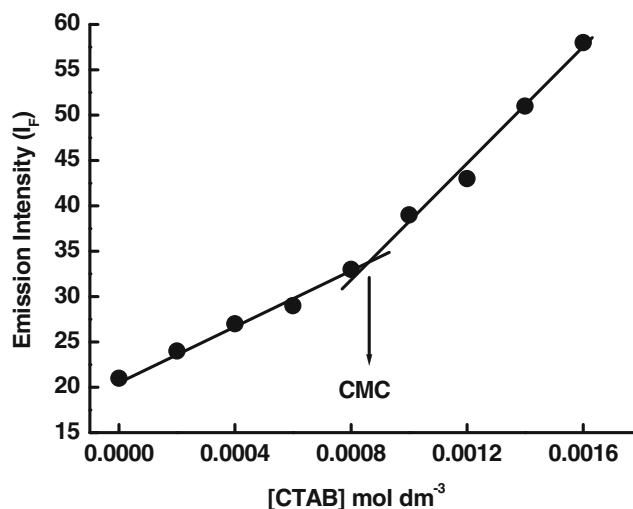


**Fig. 8** Plot of  $I_f$  versus the concentration of CTAB

aqueous bulk solution to the palisade layer of micelle. The decrease in polarity of the microenvironment around dye molecule results in the reduction of non-radiative rate from ICT state to low-lying singlet or triplet state due to the enlargement the energy gap between them, which leads to an increase in emission intensity.

## Conclusion

TMPN dye displays red shift in fluorescence spectrum as solvent polarity increases, further red shift was observed in polar protic solvents due to intermolecular hydrogen bonding between solute and solvent, the hydrogen bond with solvent enhances the radiationless processes of excited molecule. TMPN undergoes solubilization in anionic (SDS) and cationic (CTAB) micelle with abrupt change in fluorescence intensity at CMC of micelle.

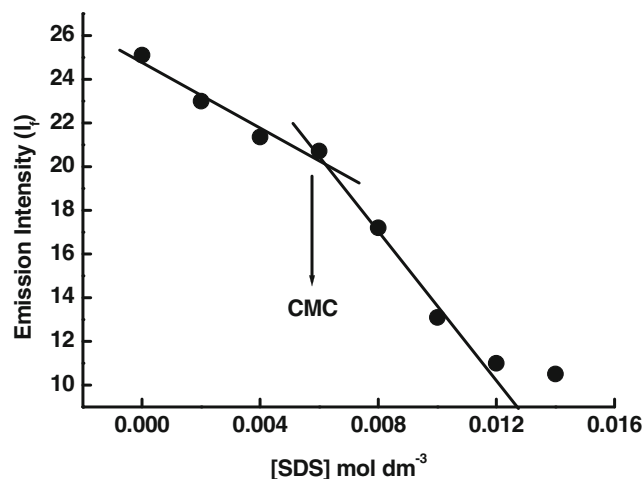


**Fig. 9** Plot of  $I_f$  versus the concentration of SDS

**Acknowledgments** The authors are thankful to the Chemistry Department at King Abdulaziz University for providing research facilities.

## References

- Wang H, Ma G, Ding Y, Lu Y, Gong S, Zhang Z, Luo H, Gao LH (2015) New armed near-IR two-photon organic chromophores undergoing ESIPT and 'naked eye' fluorescence sensing to zinc ions. *Tetrahedron Lett* 56:2758–2763
- El-Agamey A, El-Hagrasy MA, Suenobu T, Fukuzumi S (2015) Influence of pH on the decay of  $\beta$ -carotene radical cation in aqueous Triton X-100: A laser flash photolysis study. *J Photochem Photobiol B* 146:68–73
- Alwis DDDH, Chandrika UG, Jayaweera PM (2015) Spectroscopic studies of neutral and chemically oxidized species of  $\beta$ -carotene, lycopene and norbixin in  $\text{CH}_2\text{Cl}_2$ : Fluorescence from intermediate compounds. *J Lumin* 158:60–64
- Seferoglu Z, Ihmels H, Sahin E (2015) Synthesis and photophysical properties of fluorescent arylstyrylimidazo[1,2-a]pyridine-based donor-acceptor chromophores. *Dyes Pigments* 113:465–473
- Paul BK, Guchhait N (2014) Explicit spectral response of an intramolecular charge transfer molecule within microheterogeneous micellar environments. *J Mol Liq* 199:309–317
- Jiang H, Zhang J, Zhang Q, Ye S (2015) Synthesis, characterization and explosive detection of photoluminescent compounds with intramolecular charge-transfer characteristic. *Synth Met* 210:30–42
- Zhang W, Wang D, Cao H, Yang H (2014) Energy level tunable pre-click functionalization of [60]fullerene for nonlinear optics. *Tetrahedron* 70:573–577
- Wamke A, Dopierała K, Prochaska K, Maciejewski H, Biadasz A, Dudkowiak A (2015) Characterization of langmuir monolayer, langmuir–blodgett and langmuir–schaefer films formed by POSS compounds. *Colloids Surf A* 464:110–120
- Li J, Feng H, Li J, Feng Y, Zhang Y, Jiang J, Qian D (2015) Fabrication of gold nanoparticles-decorated reduced graphene oxide as a high performance electrochemical sensing platform for the detection of toxicant Sudan I. *Electrochim Acta* 167:226–236
- Roohi H, Ghauri K (2015) Exploring physicochemical properties of the nanostructured Tunable Aryl Alkyl Ionic Liquids (TAAILs). *J Mol Liq* 209:14–24
- Ray D, Nag A, Goswami D, Bharadwaj PK (2009) Acyclic donor–acceptor–donor chromophores for large enhancement of two-photon absorption cross-section in the presence of  $\text{Mg(II)}$ ,  $\text{Ca(II)}$  or  $\text{Zn(II)}$  ions. *J Lumin* 129:256–262
- Inoue S, Mikami S, Aso Y, Otsubo T, Wada T, Sasabe H (1997) Donor-acceptor-substituted heteroquinoid chromophores as novel nonlinear optics. *Synth Met* 84:395–396
- Asiri AM, Khan SA, Al-Amodi MS, Alamry KA (2012) Synthesis, characterization, absorbance, fluorescence and non linear optical properties of some donor acceptor chromophores. *Bull Korean Chem Soc* 33:1900–1906
- Muralidhar L, Girija CR (2014) Simple and practical procedure for Knoevenagel condensation under solvent-free conditions. *J Saudi Chem Soc* 18:541–544
- Khan SA, Razvi MAN, Bakry AH, Afzal SM, Asiri AM, El-Daly SA (2015) Microwave assisted synthesis, spectroscopic studies and non linear optical properties of bis-chromophores. *spectrochim. Acta A*: 137:1100–1105
- Watson BT, Christiansen EG (1998) Solid phase synthesis of substituted quinolin-2(1H)-one-3-carboxylic acids via an intramolecular Knoevenagel condensation. *Tetrahedron Lett* 39:9839–9840
- Shivashimpi GM, Pandey SS, Watanabe R, Fujikawa N, Ogomi Y, Yamaguchi Y, Hayase S (2012) Novel unsymmetrical squaraine dye bearing cyanoacrylic acid anchoring group and its photosensitization behavior. *Tetrahedron Lett* 53:5437–5440
- Asiri AM, Marwani HM, Khan SA (2014) Spectroscopic investigation of novel donor–acceptor chromophores as specific application agents for opto-electronics and photonics. *J Saudi Chem Soci* 18:392–397
- Chen R, Zhao G, Yang X, Jiang X, Liu J, Tian H, Gao Y, Liu X, Han K, Sun M, Sun L (2008) Photoinduced intramolecular charge-transfer state in thiophene- $\pi$ -conjugated donor–acceptor molecules. *J Mol Struct* 876: 102–109.
- Gilani AG, Moghadam M, Zakerhamidi MS, Moradi E (2012) Solvatochromism, tautomerism and dichroism of some azoquinoline dyes in liquids and liquid crystals. *Dyes Pigments* 92:1320–1330
- Chastrette M, Carretto J (1982) Statistical study of solvent effects—II: Analysis of some empirical parameters of solvent polarity. *Tetrahedron* 38:1615–1618
- Tsai H, Chen K (2014) Synthesis and optical properties of novel asymmetric perylene bisimides. *J Lumin* 149:103–111
- Wang B, Liao H, Yeh H, Wu W, Chen C (2005) Theoretical investigation of stokes shift of 3,4-diaryl-substituted maleimide fluorophores. *J. Lumin* 113:321–328
- Rijke E, Joshi HC, Sanderse HR, Ariese F, Brinkman UAT, Gooijer C (2002) Natively fluorescent isoflavones exhibiting anomalous Stokes' shifts. *Anal Chim Acta* 468:3–11
- Drozd M (2006) The equilibrium structures, vibrational spectra, NLO and directional properties of transition dipole moments of diguanidinium arsenate monohydrate and diguanidinium phosphate monohydrate: The theoretical DFT calculations. *Spectrochim Acta A* 65:1069–1086
- Gordon P (1987) Gregory P. Organic Chemistry in Colour. Chimia, Moskva
- Lakowicz JR (2006) Principles of Fluorescence Spectroscopy, third edn. Springer, NewYork
- Niko Y, Hiroshige Y, Kawauchi S, Konishi G (2012) Fundamental photoluminescence properties of pyrene carbonyl compounds through absolute fluorescence quantum yield measurement and density functional theory. *Tetrahedron* 68:6177–6185
- Itoh T (1999) Influence of collision on the fluorescence and phosphorescence quantum yields of benzophenone and 9,10-anthraquinone vapors. *Spectrochim Acta A* 55:273–278
- Sharma N, Jain SK, Rastogi RC (2008) Solubilization of 5-methoxy tryptamine molecular probes in CTAB and SDS micelles: A cmc and binding constant study. *Spectrochim Acta A* 69:748–756
- James J, Aellaichami S, Krishnan RSG, Samikannu S, Mandal AB (2005) Interaction of poly (ethylene oxide)–poly (propylene oxide)–poly (ethylene oxide) triblock copolymer of molecular weight 2800 with sodium dodecylsulfate (SDS) micelles: some physicochemical studies. *Chem. Phys* 312:275–287
- Li F, Li G, Wang H, Xue Q (1997) Studies on cetyltrimethylammonium bromide (CTAB) micellar solution and CTAB reversed microemulsion by ESR and  $^2\text{H}$  NMR. *Colloids Surf A* 127: 89–96.